

J. Synchrotron Rad. (1999). **6**, 217–219

The physics of ionization chambers – or how to improve your signal-to-noise ratio for transmission EXAFS measurements

Robert F. Pettifer,^{a*} Michael Borowski^b and Paul W. Loeffen^c

^a*Department of Physics, University of Warwick, Coventry CV4 7AL, United Kingdom,* ^b*European Synchrotron Radiation Facility, B.P. 220 - 38043 Grenoble Cedex, France,* and ^c*Oxford Instruments, Accelerator Technology Group, Osney Mead OX2 0DX, United Kingdom. E-mail: pettifer@trebor.phys.warwick.ac.uk*

We review the physical processes which may limit the performance of the ion chamber in making transmission EXAFS measurements. It is found that the recombination current loss is approximately proportional to the square of the saturation current and inversely proportional to the square of the applied voltage. We demonstrate the quality of data which can be achieved by measuring the rhodium K adsorption edge (T=30K and 290K) recorded at ESRF BM29, with noise levels approaching the photon counting limit. The EXAFS from this data has an error in the fine-structure function $\Delta\chi \approx 5 \times 10^{-5}$. **Keywords: ion chambers; X-ray detectors; EXAFS.**

1. Introduction

There has been an increase of at least a decade in the flux available at samples for standard transmission EXAFS measurements as a result of the improvements accompanying each new generation of synchrotron source. Unfortunately, this may not be reflected in improvements in signal to noise ratio of the data recorded. Furthermore, the usually attained noise is above the theoretical photon counting limit $\Delta s = \sqrt{1/N + 1/N'}$; where s is the absorption thickness product μx and N and N' are the number of photons absorbed in the front and rear detectors respectively. Assuming that the photons are equally divided between the incident and transmitted detector then if $s \approx 1$ (chosen to minimize thickness effects from the tails of the monochromator) then $\Delta s/s \approx \sqrt{2(1+e)/I_0 t} \approx \Delta\chi$, where χ is the fine structure function. At BM29 of the ESRF, for example, (currently an unfocussed beamline), the measured flux I_0 available in a 3eV bandwidth provided by a Si(111) monochromator 40% detuned, over an area of 0.5×6 mm at 23KeV and with the ESRF at 6GeV and 57mA beam current is 3×10^9 photons per second. This give a photon counting $\Delta\chi \approx 4 \times 10^{-5}$ for a two second integration time.

We discuss the basic physics of ion chambers, and treat in detail the recombination process in the next section. A list of possible interference sources that we have encountered and their remedies which limit data quality is given in section 3. Finally, we present an EXAFS measurement to illustrate the data quality attainable.

2. Basic Physics of Ion Chambers

The ionisation chamber has been extensively investigated as a radiation detector over many years (Rossi & Staub, 1949; Sharpe, 1964; Knoll, 1979). The model used for the ionisation process is

that x-rays enter the chamber and undergo a localized absorption event at a gas atom. The annihilation of the x-ray photon releases energy in the form of secondary ion electron pairs and it is found that the energy required to produce an ion electron pair w is a constant over a wide range of photon energies and is a function of the gas in the chamber. Values of w are 27.8eV (He), 27.4eV (Ne), 24.4eV (Ar), 22.8eV (Kr), 20.8eV (Xe) (Vaughan, 1986). Ions and electrons are drawn apart via a field which in our case is formed by a voltage applied to two parallel metallic plates separated by 30mm. The ions have a well defined drift mobility for pure gases whereas electrons accelerate until they acquire sufficient energy for gas excitation (inelastic collisions) to occur. With an applied maximum voltage of 3KV and 1 Atm of Ar the ion drift velocity is 15 m/s, and the electron drift velocity is 2×10^4 m/s with the velocity varying more slowly than linearly with voltage (Sharpe, 1964).

The ion-electron weak plasma is not closely confined to the region of the gas exposed to the X-ray beam, but is spread over a volume which depends on composition and pressure of the gas, and the X-ray photon energy. The extent of ionisation is controlled by the migration of the hot Auger and photoelectrons. In 1 Atm Ar at 3KeV the hot electron range is 17mm (Charpak *et al.*, 1978).

If a mixture of the gas is used then the ionisation current is strongly related to the gas component with the smallest ionisation energy, as excited states are most readily de-excited via ion gas collisions. Since the number of collisions expected for an ion in its drift time is $\approx 10^6$ only a small quantity ($\leq 0.1\%$) of low ionisation energy gas is required to maximize the number of ion pairs per photon.

Similar considerations apply in discussing electron transport. Some gases, notably O_2 and H_2O have large electron capture probabilities ($\approx 10^{-3}$) and the presence of small quantities of these gases drastically affect the drift velocity of negative charge and indirectly alter the recombination coefficient which enhances non-linearity in the chamber. All rare gases, nitrogen, and the saturated hydrocarbons have zero electron capture cross-section. An estimate of electron collision frequencies from simple kinetic theory indicates that the electron may undergo 10^5 collisions prior to collection at the anode. Thus to minimize electron attachment, water and oxygen concentrations should thus be $\leq 10^{-4}$. These conditions can be maintained using high vacuum sealed chambers for a few days before refilling becomes necessary.

At low applied voltages to the plates of the ion chamber, space charge effects, created by the slow moving ion sheath (Hemenway *et al.*, 1962), may be considered small when the free charge stored on the capacitor plates of the chamber $Q(\approx 10^{-8}C) \gg q(\approx 10^{-11}C)$, the positive ion charge in transit. (Field lines must begin and end on charges). These conditions are easily met by applying a few hundreds of volts to the chamber when the ion current is less than 100nA.

2.1. Recombination Non-linearity

At applied voltages which are higher than those necessary for removal of space charge effects, the chamber characteristics reach a saturation plateau, where the chamber is normally operated. On close examination in this region, the current continues to increase with applied voltage. The increase is caused by the reduction of recombination which removes charge created by the photon, and thus cannot contribute to the ionisation current. The recombination rate is essentially of the bi-molecular type, and is proportional to the product of the local concentration of +ve and -ve charge carriers $\rho_+ \rho_-$. Under steady state conditions the local concentration

ρ will also be inversely proportional to the speeds v of the carriers. Furthermore, if well defined mobilities exist for the carriers, then the speeds will be proportional to the applied voltage V . Thus $\rho \propto V^{-1}$. Under these circumstances, we can postulate the phenomenological expression for the measured current,

$$i = i_s - k \frac{i_s^2}{V^2} \quad (1)$$

where i and i_s are the measured and saturation currents, and k is a constant independent of current and voltage which depends on the plate separation, the type, pressure, and purity of the gas, and the energy of the photon beam. In writing Eqtn. 1 we have exploited the proportionality between the charge density ρ and the saturation current i_s . We have tested Eqtn. 1 with a series of current voltage characteristics. In testing this relation we have been wary of the weak assumption of the existence of an electron mobility, and initially have allowed the exponents of i_s and V to vary. It was found that the exponent of voltage was 1.98 ± 0.03 , and an exponent of current of 1.95 ± 0.05 . Thereafter the exponent of voltage was fixed at 2, and only the exponent of current was allowed to vary. A comparison of this version of Eqtn. 1 and experiment is displayed in Fig. 1, where the fractional recombination current loss $(i_s - i)/i_s$ is plotted against V^{-2} . We find that k , in Eqtn. 1 is $43 \pm 3(V^2(\text{nA})^{-1})$ and the exponent of current is $1.93 \pm 0.05 \approx 2$.

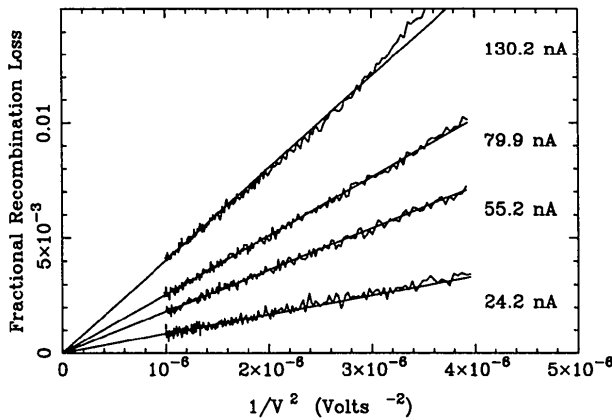


Figure 1 Fractional recombination loss plotted as a function of $1/V^2$ for differing ionisation chamber saturation currents. The straight lines are as predicted by Eqtn. 1.

To establish the absorption thickness product normally requires measuring the ratio of the ionisation chamber currents both with and without a sample, and taking a log of the ratio. For many EX-AFS measurements the "without sample" measurement is omitted and we will follow this convention for the sake of simplicity and write for the observed absorption coefficient μ_{obs} ,

$$\mu_{obs} \propto \log \frac{i}{i'} = \log \left(\frac{i_s (1 - k i_s / V^2)}{i'_s (1 - k' i'_s / V^2)} \right), \quad (2)$$

where the unprime and prime characters refer to the first and second ionisation chambers respectively. Assuming $k i_s V^{-2} \ll 1$ then

$$\mu_{obs} \approx \mu + (k' i'_s - k i_s) V^{-2}. \quad (3)$$

It is clear from Eqtn. 3 that the observed absorption coefficient is dependent on the saturation currents, and thus on the intensity of

the beam. Intensity variations can occur for a variety of reasons and these will be recorded as apparent fluctuations in the absorption coefficient via the second term of Eqtn. 3. The causes of the intensity variation can include: electron orbit instability; the monochromator can yield a variation of output owing to the presence of simultaneous reflections; or the feedback mechanism on the crystal detuning can vary throughout the course of a scan. To achieve optimum results k must be made as small and V large, or under extreme conditions, it may be possible to correct for, or to null the first order non-linear term.

2.2. Interference sources

The aforementioned factors are calculable and relatively well understood, but other factors are not calculable, and are frequently more important. In our experience, the most important factor in achieving low noise data is the elimination of ground loops which may flow in the shielding cable of the amplifier. The main countermeasure for this type of interference is to electrically isolate the ion chamber from the beam-line.

The second most important source of interference comes from microphony. This can appear from the chamber itself or equally from the amplifier cable. The problem can be particularly severe when vacuum pumps operate close to the beam-line with stainless steel bellows which can resonate. The problem is minimized by vibrational isolation, the use of rigid tube construction of the body and electrodes and low microphony cable (made as short as possible).

The third source of interference comes from charging of insulators in the body of the detector. This is eliminated in the design by shielding all insulators from the source of free charges.

The fourth source of interference comes from the high voltage power supplies which may possess an ac component which can capacitively couple to the amplifier. Many amplifiers have restricted band-width imposed at an output stage, and so the experimenter may be unaware of over-load problems in the front end electronics. As a further counter measure, the use of identical size chambers matches the chamber capacitances, and some cancellation results if the extraction fields are sourced from the same supply.

A fifth type of noise may come from the amplifier itself, however with modern ultra low bias current front end operational amplifiers the noise is dominated by the current to voltage feed-back resistor and temperature stability (Burr-Brown, 1994). Assuming that the transimpedance is 10^9 volts per amp then the resistor noise integrated over one second is $4 \times 10^{-6} V / \sqrt{\text{Hz}}$. To achieve input bias and offset stability of 100fA requires a typical temperature stability of $\approx 10^\circ \text{C}$.

3. Results

The X-ray absorption spectrum of rhodium foil was measured at 30K and 290K using approximately 3000 points and integrating for 2 seconds per point. Ion chamber currents were $\approx 100\text{nA}$ and were filled with Ar at 1 and 2 Atm. The length of the charge collection plates was 300mm and a voltage of 1KV was applied across a 30mm gap. Novelec medium sensitivity amplifiers (Gauthier *et al.*, 1995) operating in the unchopped mode were used. The amplifiers had an integral voltage to frequency converter, which was optically coupled to the counting system, and set such that a 300nA input current produced 10MHz output count rate. The maximum variation in the incident flux was 10% over the course of the scan.

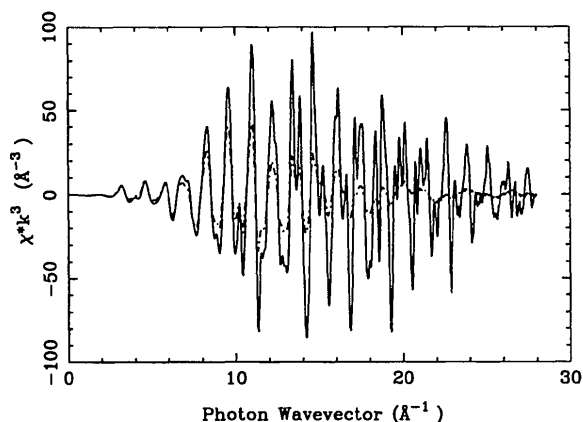


Figure 2
The k^3 weighted EXAFS for rhodium metal measured at 290K (dashed) and 30K (full)

A pre-edge fit to an energy power law was applied, followed by a post edge multi-interval spline. This produced the k^3 weighted fine structure shown in Fig. 2. No smoothing editing or filtering has been applied to this data. The origin of k , the photoelectron wavevector is set at the maximum of the first derivative of $\mu(E)$. Fine structure is seen to 28 \AA^{-1} , and an estimate of the noise yields $\Delta\chi \approx 5 \times 10^{-5}$.

4. Discussion

We have reviewed a fundamental source of non-linearity of ionisation chambers and shown the importance of using the maximum

chamber voltage. We have found that a V^{-2} relationship is obeyed for a typical Ar filling. This is a surprise in view of the non-linear electron drift velocity with field. The fractional recombination loss is a factor of 20 smaller than that calculated by Colmenares (1974), even though our active volume was also a factor 5 smaller. It is possible that our recombination loss is still dominated by small concentrations of impurity. Nevertheless we have recorded an EXAFS spectrum which shows noise levels comparable to that expected on the basis of photon counting statistics.

We would like to acknowledge useful discussions with R. Weigel and M. Kocsis. One of us (RFP) would like to thank Oxford Instruments for financial support to attend the XAFS X conference.

References

- Burr-Brown IC Applications Handbook* (1994), 167-171, Burr-Brown, Tucson.
 Charpak G., Sauli F. & Kahn R. (1978). *Nucl.Inst.Met.* **158**, 185-190
 Colmenares C. A. (1974). *Nucl.Inst.Met.* **114**, 269-275.
 Gauthier C., Goujon G., Feite S., Moguiline E., Braicovich L., Brookes N.B. & Goulon J. (1995). *Physica B* **208/209**, 232-234
 Hemenway C.L., Henry R.W. & Caulton M. (1962). *Physical Electronics*, 188, Wiley, New York.
 Knoll G. F. (1979). *Radiation Detection and Measurement*, 151-173, Wiley, New York.
 Rossi B. B. & Staub H. H. (1949). *Ionisation Chambers and Counters*, 1-243, McGraw-Hill, New York. Wiley, New York.
 Sharpe J. (1964). *Nuclear Radiation Detectors*, 1-103, 154-162, Methuen, London.
 Vaughan D. (Ed) (1986). *X-ray Data Booklet*, 6-2, Center of X-ray Optics, Lawrence Berkeley Laboratory, Berkeley.

(Received 10 August 1998; accepted 12 January 1999)